RL-TR-97-254
In-House Report
April 1998
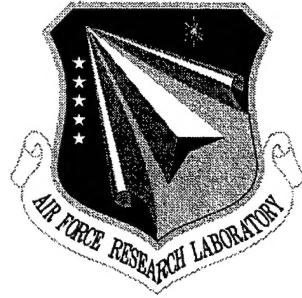
BLUE/UV EMITTING GaN LASER

Capt William A. Davis

19980512 005

**AIR FORCE RESEARCH LABORATORY
ROME RESEARCH SITE
ROME, NEW YORK**

DTIC QUALITY INSPECTED 3

This report has been reviewed by the Air Force Research Laboratory, Information Directorate, Public Affairs Office (IFOIPA) and is releasable to the National Technical Information Service (NTIS). At NTIS it will be releasable to the general public, including foreign nations.

RL-TR-97-254 has been reviewed and is approved for publication.

APPROVED:

FRANZ HAAS, Acting Chief
Photonics Processing Branch

FOR THE DIRECTOR:

GARY D. BARMORE, Maj, USAF
Chief, Rome Operations Office
Sensors Directorate

REPORT DOCUMENTATION PAGE		Form Approved OMB No. 0704-0188

Public reporting burden for this collection of information is estimated to average 1 hour per response, including the time for reviewing instructions, searching existing data sources, gathering and maintaining the data needed, and completing and reviewing the collection of information. Send comments regarding this burden estimate or any other aspect of this collection of information, including suggestions for reducing this burden, to Washington Headquarters Services, Directorate for Information Operations and Reports, 1215 Jefferson Davis Highway, Suite 1204, Arlington, VA 22202-4302, and to the Office of Management and Budget, Paperwork Reduction Project (0704-0188), Washington, DC 20503.

1. AGENCY USE ONLY *(Leave blank)*	2. REPORT DATE April 1998	3. REPORT TYPE AND DATES COVERED In-House Oct 96 - Dec 97	
4. TITLE AND SUBTITLE BLUE/UV EMITTING GaN LASER			5. FUNDING NUMBERS C - N/A PE - 62702F PR - 4600 TA - P1 WU - 32
6. AUTHOR(S) Capt William A. Davis			
7. PERFORMING ORGANIZATION NAME(S) AND ADDRESS(ES) Air Force Research Laboratory/SNDP 25 Electronic Parkway Rome NY 13441-4515			8. PERFORMING ORGANIZATION REPORT NUMBER RL-TR-97-254
9. SPONSORING/MONITORING AGENCY NAME(S) AND ADDRESS(ES) Air Force Research Laboratory/SNDP 25 Electronic Parkway Rome NY 13441-4515			10. SPONSORING/MONITORING AGENCY REPORT NUMBER RL-TR-97-254
11. SUPPLEMENTARY NOTES Air Force Research Laboratory Project Engineer: Capt William A. Davis/SNDP/(315) 330-2015			
12a. DISTRIBUTION AVAILABILITY STATEMENT Approved for public release; distribution unlimited			12b. DISTRIBUTION CODE

13. ABSTRACT *(Maximum 200 words)*

This report presents results from an epitaxial growth study of Gallium Nitride (GaN) for use as ultraviolet (UV) and blue laser diodes and light emitting diodes (LEDs). The method of growth investigated was Molecular Beam Epitaxy (MBE). The group V source was nitrogen gas that was cracked utilizing a 13.56 MHz Radio Frequency (RF) plasma source. From this RF plasma, sufficient atomic nitrogen was produced to obtain growth rates of GaN of $>0.65 \mu m/hr$. Both n- and p-type wurtzite GaN was grown on basal plane sapphire substrates. In addition, results from growth attempts on cubic-SiC substrates is described. Results from photoluminescence spectroscopy (PL), Hall effect measurements, and Atomic Force Microscopy (AFM) of samples are shown and their effect on resulting changes in the growth recipe. Finally, results from the growth of $Al_{(x)}Ga_{(1-x)}N$ are presented.

14. SUBJECT TERMS Gallium Nitride, Molecular Beam Epitaxy (MBE), Blue Laser, Light Emitting Diodes (LEDs)			15. NUMBER OF PAGES 44
			16. PRICE CODE
17. SECURITY CLASSIFICATION OF REPORT UNCLASSIFIED	18. SECURITY CLASSIFICATION OF THIS PAGE UNCLASSIFIED	19. SECURITY CLASSIFICATION OF ABSTRACT UNCLASSIFIED	20. LIMITATION OF ABSTRACT UL

Standard Form 298 (Rev. 2-89) (EG)
Prescribed by ANSI Std. 239.18
Designed using Perform Pro, WHS/DIOR, Oct 94

TABLE OF CONTENTS

LIST OF FIGURES

ACKNOWLEDGEMENTS

ABSTRACT

This report presents results from an epitaxial growth study of Gallium Nitride (GaN) for use as ultraviolet (UV) and blue laser diodes and light emitting diodes (LEDs). The method of growth investigated was Molecular Beam Epitaxy (MBE). The group V source was nitrogen gas that was cracked utilizing a 13.56 MHz Radio Frequency (RF) plasma source. From this RF plasma, sufficient atomic nitrogen was produced to obtain growth rates of GaN of >0.65 μm/hr. Both n- and p-type wurtzite GaN was grown on basal plane sapphire substrates. In addition, results from growth attempts on cubic-SiC substrates is described. Results from photoluminescence sprectroscopy (PL), Hall effect measurements, and Atomic Force Microscopy (AFM) of samples are shown and their effect on resulting changes in the growth recipe. Finally, results from the growth of $Al_{(x)}Ga_{(1-x)}N$ are presented.

INTRODUCTION

The potential of III-Nitride materials for device applications has been widely recognized with the successful demonstration of blue lasers[1,2] as well as highly efficient light emitting diodes (LED's)[3]. In addition to the success of optical devices, GaN based Field Effect Transistors FET's have demonstrated excellent high frequency performance showing cutoff frequency (f_T) of 36.1 GHz[4] and maximum oscillation frequency (f_{max}) of 77 GHz[5].

To achieve the III-Nitride based LED's at Cornell University, the growth of nitride films using Gas Source Molecular Beam Epitaxy (GSMBE) and processing of nitride materials has been studied. In this report, the results achieved through process developments and material growths are presented. The process developments were made on etching and Ohmic contacts of III-V nitrides while high optical quality GaN growth by MBE was achieved.

The growth of GaN presents many difficulties to the crystal grower due to the lack of a lattice matched substrate such as bulk grown GaN. Instead, the grower is forced to use substrates that are mismatched in both lattice constant and thermal conductivity. The disadvantage of this is that both issues cause on the order of 10^{10} cm^{-2} threading dislocations in the GaN epilayer grown on a mismatched substrate. Another problem that must be overcome before LEDs and laser diodes can be made is the reduction in the background n-type carrier concentration. For MBE epilayers of GaN, a typical background intensity would be n=1.0 E10^{17}cm^{-3}. This high background density makes it difficult to grow conductive p-type GaN due to acceptor compensation from the n-type background. In this report, methods used to reduce both the dislocations and the n-type background are introduced. It is remarkable that today highly efficient and long lifetime LEDs have been grown and fabricated let alone laser diodes from this "defective" material.

For the fabrication of laser diodes (LD's) and LED's, it is imperative to have smooth side walls for mirror facets and light wave guides. Due to the hexagonal structure of nitride films that has no convenient cleavage planes like GaAs, side walls must be achieved through etching.[6] Yet the difficulty is more severe due to the durability of the crystal structure. The tolerance of smoothness is smaller for nitride optical devices than for the other compound semiconductors because of the short wavelength of light that a nitride device generates. If the tolerance is 1/16 of

1

the wavelength, a side wall of GaN must be made within 23 nm in fluctuation from peak to peak assuming an emission wavelength of 368 nm. Etching has been a problem with nitrides due to their robust structures. In many research groups, the etching of III-Nitrides is mostly done using reactive ions and /or ion beams, such as Reactive Ion Etching (RIE), Electron Cyclotron Resonance Etching (ECR), and Chemically Assisted Ion Beam Etching (CAIBE). There are no known wet chemical etches for GaN. An AZ photoresist developer is known to etch AlN selectively.

Another problem to overcome in achieving high performance GaN-based devices is the realization of good reliable metal contacts. The strong crystal bonds of III-Nitrides also imposes a difficulty in making good Ohmic contacts. For as-deposited metal contacts on highly doped semiconductors, tunneling current dominates the total current. The specific contact resistance is roughly determined by the tunneling mechanism. Contact resistance, r_c, is determined from the following equation.[7]

$$r_c \sim \exp\left[\frac{2\phi_B}{\hbar}\sqrt{\frac{\varepsilon_s \cdot m^*}{N_D}}\right]$$

Thus a high doping density in a semiconductor will yield an Ohmic contact with low contact resistance. A high doping concentration can be obtained by intentionally doping during growth or by introducing dopants from overlay metals through an annealing process or RIE processes.[8] In nitrides, higher temperatures are required for dopant diffusion than in GaAs or InP. However, metal-semiconductor junction destruction would probably be occurring through the chemical reaction normally taking place during the high temperature anneal, making the contacts highly resistive.

2

MBE GROWTH of GaN

Bandgap and Lattice Constant

The only direct bandgap semiconductors which can emit light in the UV wavelength regions are the III-nitrides; GaN and compounds of $Al_{(x)}Ga_{(1-x)}N$ and $In_{(x)}Ga_{(1-x)}N$. A diagram showing the bandgap and emission wavelength dependence of the III-nitrides as a function of lattice constant is shown in Figure 1. These wide bandgap materials are also employed in high temperature electronics. There is a significant difference in the manner of change in bandgaps of the III-nitrides compared to the more conventional III-arsenide semiconductors. AlN is significantly lattice mismatched to GaN while AlAs is nearly lattice matched to GaAs. As a result, it is not possible to grow very thick clad layers of AlN on GaN without generating lattice defects to accommodate the difference in lattice constants. It is very difficult to make lateral cavity lasers with sufficient optical confinement for good efficiency when constrained to the thickness presented in the AlGaN materials system. Two forms of GaN, AlN and InN can exist.
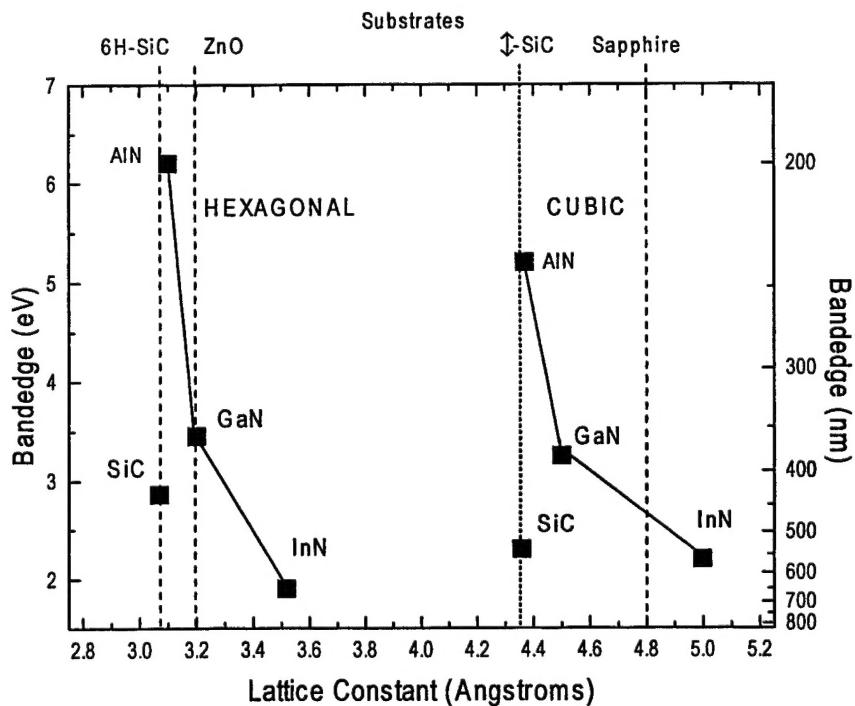
Figure 1: Bandgaps and Lattice Constants for Wurtzite and cubic III-nitrides

These are wurtzite (hexagonal) structures, or they can exist as zincblende (cubic) forms. The most common forms of these materials are the wurtzite structures. Cubic nitrides are more difficult to synthesize as a practical matter because lattice matched cubic substrates do not exist. It can be seen that the bandgap of hexagonal GaN corresponds to a wavelength of approximately 364 nm in the UV. Alloys of AlGaN move the bandgap to higher energies where emission wavelengths closer to 300 nm and shorter appear possible.

Growth of GaN by MBE

All GaN materials grown for this study came from a molecular beam epitaxy (MBE) machine which has been configured during this study for growth of nitrides. A schematic of the MBE machine is seen in Figure 2. Conventional thermal sources are used for the group III elements and dopants. Nitrogen gas cannot be directly used for GaN growth. Nitrogen (N_2) must be dissociated prior to reaching the surface of the substrate in order to incorporate in GaN. The technique used in this study to break the nitrogen molecule was the application of 13.6 MHz RF
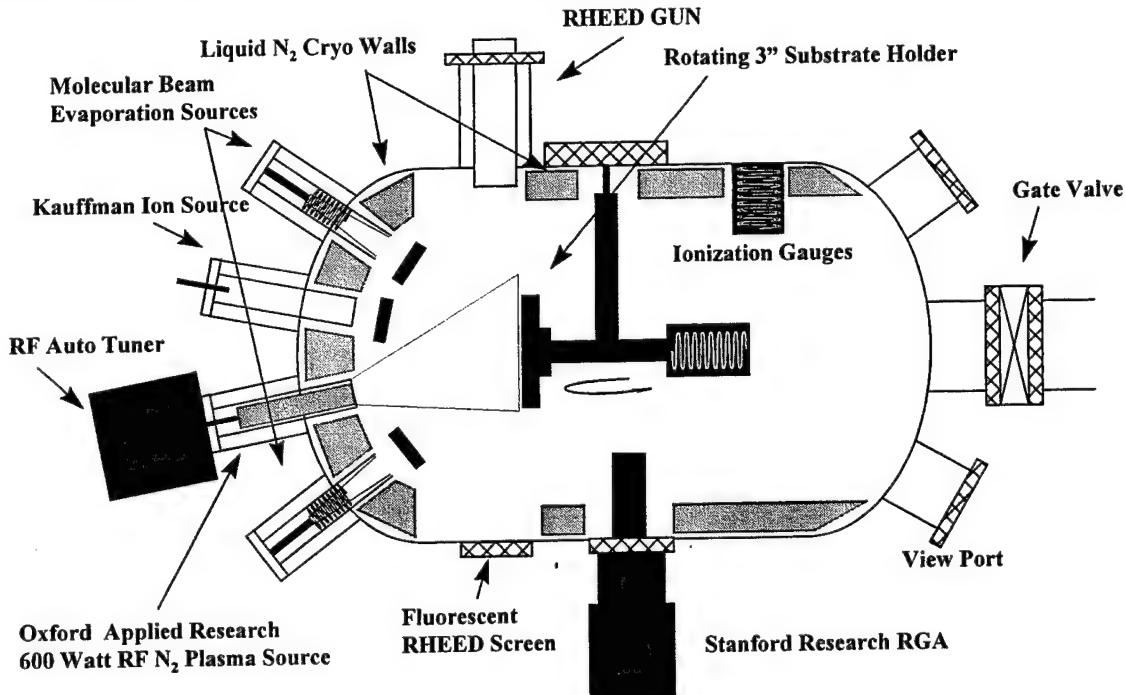
Figure 2: Diagram of MBE machine used for the growth of III-Nitrides at Cornell.

4

energy to form a nitrogen plasma in an atomic nitrogen source assembly which has an opening that faces the substrate. A fraction of approximately 6-8% of the gas which enters the remote RF plasma source will exit as atomic nitrogen. The plasma source is an Oxford Instruments model Cars-25. The majority of nitrogen will enter the chamber as N_2. Since it cannot be used for growth of GaN, it must be rapidly removed to avoid degrading the desired growth process. A 2400 l/sec turbomolecular pump efficiently removes unreacted N_2 from the chamber and keeps the pressure in the range of low 10^{-5}T while N_2 is flowing in at a rate of 2-3 sccm. The drawbacks to using a turbomolecular pump include oil backstreaming from oil-based roughing pumps, and the possibility of catastrophic failure of internal seals which can rupture and fill the chamber with turbo pump oil. This mode of failure did occur during November 1995. The problem was repaired and no contamination of GaAs films was subsequently detected. It is presumed that GaN was similarly unaffected by the failure, but the possibility remains that the results of this study have been affected in ways that are not evident at the present time.

An additional concern when employing source gas in a MBE machine is the possibility of contamination of the growth environment through source gas impurities. Oxygen is normally to be avoided in MBE growth of semiconductors. The starting point for high purity nitrogen gas used in this facility is employment of boil-off gas from a liquid nitrogen tank as a nitrogen source. This is one of the highest purity starting gases available. Following standard ultra-high purity practices, the gas enters the MBE gas cabinet where it is further purified by commercial resin filters. An additional point of use resin filter is used just before gas enters the RF plasma source. The Kaufman ion source seen in Figure 2 has not been used extensively to date. It will be used in future studies of the growth of GaN. The Mg and Si dopants will be discussed later in this section.

Remote RF plasma source of atomic nitrogen
Atomic nitrogen present in the source can be monitored through the observation of the optical spectrum of the plasma glow. Optical filters to reject all wavelengths of light except those that come from atomic nitrogen transition lines are used in front of an optical detector. The detector output is directly proportional to the amount of atomic nitrogen present in the plasma. The atomic nitrogen signal is dependent on RF power and the amount of nitrogen that is injected into

the source. A plot of the atomic nitrogen signal as a function of power and amount of nitrogen (measured as MBE chamber pressure) is seen in Figure 3.
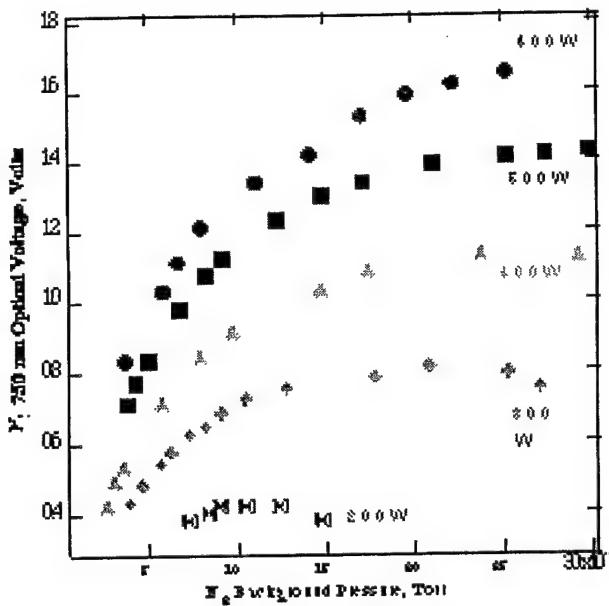
Figure 3: Optical signal corresponding to atomic nitrogen is shown as a function of RF power and MBE chamber pressure.

The curve does not show the limited range in pressure over which a plasma can be struck, or ignited, at each power level. The plasma will only turn on within a narrow band of pressure somewhere within the center of each curve shown. The band is widest for highest RF power and narrower for low power. If the plasma is operated outside of this strike range and should go out, it will not restart without intervention to change pressure back to the strike range.

Another aspect of plasma operation is source temperature. The source is designed to be cooled by a large flow of cold N_2 gas. The source of gas is LN_2 which is warmed through a heating coil to enter the source at a temperature of approximately -20°C. The amount of LN_2 consumed dictates that the source must be fed from a large outdoor tank to be operational for periods about a day or more without interruption. In practice, it is very difficult to regulate the flow of nitrogen gas to the source because the vacuum jacketed delivery system is shared by the LN_2 phase separator used to cool the MBE machine. The pressure variations in this system are so great that a solenoid in the gas line to the RF source must be controlled by a thermocouple in the source. Although this system works for the majority of conditions encountered, there are times when pressure transients cause the source to become too hot for safe operation, or so cold that the

6

plasma is extinguished. Between 25 and 50% of all growth starts were ruined when the plasma went out. Some improvement could be seen by being careful to keep the plasma pressure within the strike range, but reliable operation remains a topic of development. For this reason, this commercial plasma source would not be recommended for new programs involving the MBE growth of GaN unless extensive measures are taken to solidify plasma stability.

A near catastrophic failure of the Oxford CARS-25 source occurred approximately 18 months after installation. The gas feed line broke in two pieces during operation. The effect of this failure was to bring the MBE chamber up to atmospheric pressure instantly. Fortunately, the gas which leaked into the chamber was N_2 from the cooling gas which surrounds the gas line inside of the cooling chamber portion of the source. The source furnaces do not appear to have been damaged from the instant atmospheric pressure contamination, however no new growths have been made as of March 1997 to confirm that no damage has taken place.

The cause of the failure would appear to be a result of coupling stray RF from the feed going to the plasma RF coil into the gas line. The precaution which is designed to avoid this problem is to keep the gas line isolated from ground at both ends by ceramics. At the discharge tube side, the gas line is insulated through its metal to ceramic seal. At the gas entrance side, the gas line is isolated through a series ceramic connection. It is our best guess that contamination of the cooling gas components carried enough of some sort of conducting deposits (metal filings, etc) onto the ceramic spacer to cause it to short out and increase its coupling of RF energy. A current maximum in the standing wave was then sufficient to melt the stainless gas feedline.

Due to the failure and the slow growth rate achieved, another RF plasma source was ordered from EPI MBE Products Group. This source has made many improvements to increase the cracking efficiency of N_2 gas. It has been reported that over 90% of the gas entering the source is converted into atomic nitrogen. Growth rates as high as 0.65 μm/hr have been reported at 450 Watts. In addition, the stability has been improved by moving to an integrated water cooling system for the RF coil. The use of this source improved the ability to grow thick films in shorter times and produce higher quality GaN. Unfortunately, this source also failed internally due to the cooling system. A blockage of the integrated cooling wire forced a break in the RF coil which leaked water with glycol mix directly into the chamber. The MBE machine has been down for repairs since this time and no growths have been attempted.

Substrate mounting techniques

Sapphire was used almost exclusively as the substrate for GaN growth. Sapphire was mounted to molybdenum (moly) substrate blocks using indium as a solder. This is the technique which had been employed for almost 20 years for mounting small substrates for MBE growth. Sapphire was prepared in three configurations for these growths. A one inch substrate would be used whole, or cut in half, while 2 inch substrates were cut into quarters and only a quarter would be used at a time. These smaller pieces were used to minimize substrate costs. These smaller pieces would then be mounted to the moly block with indium in the same fashion as used previously for GaAs.

The excellent thermal contact offered by indium solder has been helpful towards minimizing one problem in the control of substrate temperature in MBE. The substrate is very close in temperature to the temperature of the moly block. This helps to identify the actual temperature of the substrate itself. The block is not in direct contact with the substrate heater station thermocouple. The thermocouple is radiatively heated by the back of the moly block. Unfortunately, the thermocouple receives some heat from the heater filaments which raises the thermocouple temperature above that of the moly block. A comparison between the thermocouple temperature and the moly block/substrate temperature measured by a pyrometer is seen in Figure 4. It can be seen that the thermocouple temperature is approximately 200°C hotter than the actual substrate temperature. Although all reports of temperature in this effort are those measured by the thermocouple, it can be seen that actual temperatures are lower. The difference
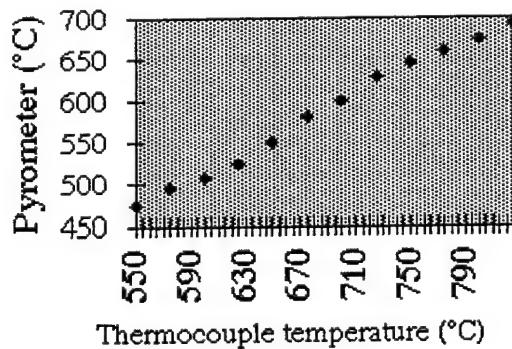

Figure 4: Comparison of substrate thermocouple temperature and substrate temperature measured by a pyrometer.

between the actual and the control temperature can vary widely between different laboratories. These differences make it difficult to utilize conditions reported by other labs without undergoing the expensive process of formulating parameter variation curves to establish similar relationships.

Although indium mounting provides excellent heat transfer from the moly block to the substrate, it has a disadvantage for the growth of GaN that is often not seen for GaAs growths. GaN grows at slow growth rates ($0.1\mu m$ to $0.2\mu m$ per hour) compared to GaAs (1.0 μm per hour). As a result, typical growths take 5 to 10 times longer sometimes lasting for more than one day. During these long times, the substrate is held at temperatures of approximately 700°C and an initial substrate nitridization occurs at approximately 800°C. At these long times and high temperatures, significantly more Indium solder evaporates away from between the substrate and moly block than occurs for GaAs. The effects of this evaporation are very harmful to GaN growth.

When indium evaporates, the thermal contact between the moly block and substrates becomes smaller and the substrate surface temperature falls while the moly block temperature is held constant by the control thermocouple. Substrate temperature is an important parameter in controlling the quality of GaN as shown later in this report. As a result of falling substrate temperature, the growth conditions change so much during a long growth that the material quality varies with depth and is poorest at the surface. It becomes very difficult to develop techniques to optimize material quality under these conditions. In addition, approximately one wafer out of every four grown will fall off the moly block because too much indium solder evaporates.

These difficulties took several months to uncover, however the solution which was reached has been very valuable to reproducibility of GaN growth. The new method of mounting substrates is seen in Figure 5. The wafer is held by clips between a backing plate and front plate. The backing plate has a cutout of the same shape and size as the substrate. This permits heat from the heaters to directly radiate onto the substrate.

9
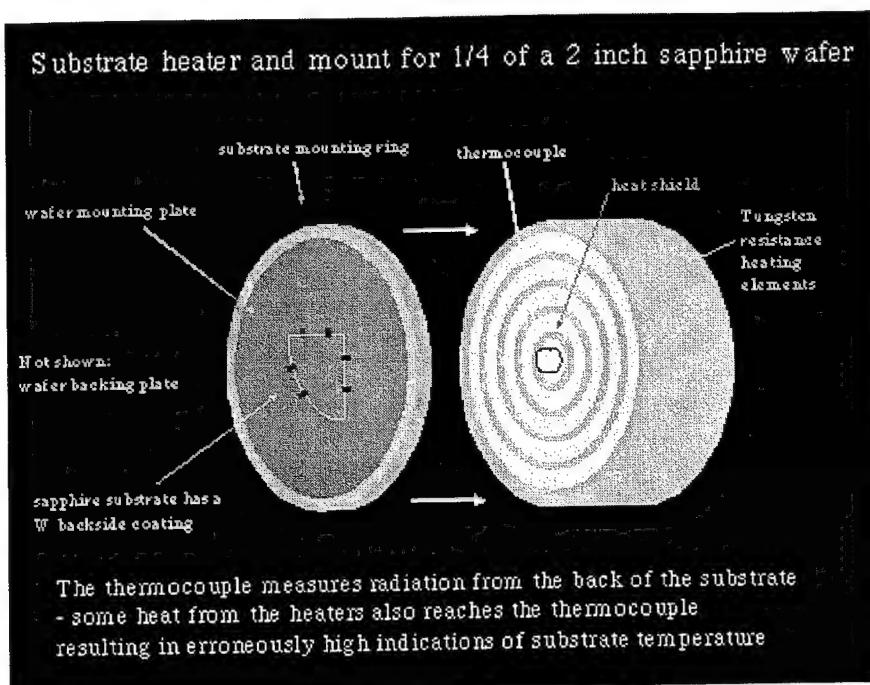
Figure 5: Indium free method of mounting wafer slices for GaN growth.

The new substrate mounting technique presents a new problem. The blackbody radiation from the heaters largely passes through the transparent sapphire substrate. In order to raise the actual substrate temperature to a given value, the heaters must be set to much higher power than was used for the indium substrate mounting. This is undesirable for a number of reasons. The higher power will produce more outgassing of unintentional background gases from the hotter substrate heater mechanism. These gases can contaminate the purity of the growing GaN wafer. The higher power will also shorten the lifetime of the substrate heater filament, and will establish a smaller upper limit to maximum substrate temperatures that can be reached. For these reasons, the substrates are metallized with tungsten, and prepared with roughened backsides to increase radiative heat absorption. If the substrate is not roughened prior to metallization, the metal will resemble a mirror and reflect significant amounts of heat back to the heaters rather then transfer the heat to the substrate. Using this technique, it is possible to obtain pyrometer measurements of substrate temperature that are very close to those of indium bonded substrates.

Another problem noted with the piece mounting system was the top plates with the retaining clips became very brittle and prone to breakage under the high temperatures and exposure to RF nitrogen plasma. Thus, the moly top piece was replaced with a similarly shaped piece made of

10

Boron Nitride. This proved to be a significant improvement with the number of wafers lost to slippage almost eliminated.

Reflection High Energy Electron Diffraction of GaN

An important element of GaN growth by MBE is the ability to monitor the growing surface using reflection high energy electron diffraction (RHEED). The RHEED reconstruction seen on a phosphor screen can give indications about the relative quality of the growing surface. It has been useful to identify the type of GaN crystal lattice also. It is clear from RHEED when GaN is a wurtzite form, or a cubic form. Some cubic GaN was grown for this effort on cubic SiC which clearly showed cubic symmetry. When GaN was grown on GaAs, the RHEED pattern did not show only cubic symmetry, but instead a combination of cubic and wurtzite phases were observed. This is an important observation because X-Ray diffraction of GaN grown on GaAs often is more sensitive to the cubic phase of the material and has lead to many false reports of cubic GaN on GaAs.

RHEED observations of GaN growth begin with observation of the sapphire substrate. The RHEED reconstruction from a typical sapphire substrate is seen in Figure 6. The horizontal lines indicate that the surface consists of a regular pattern of atoms. The RHEED reconstruction can be thought of in terms of the reciprocal of the surface atom arrangement. A regular flat array of atoms will be transformed in appearance to an array of lines while a non-flat array will give rise
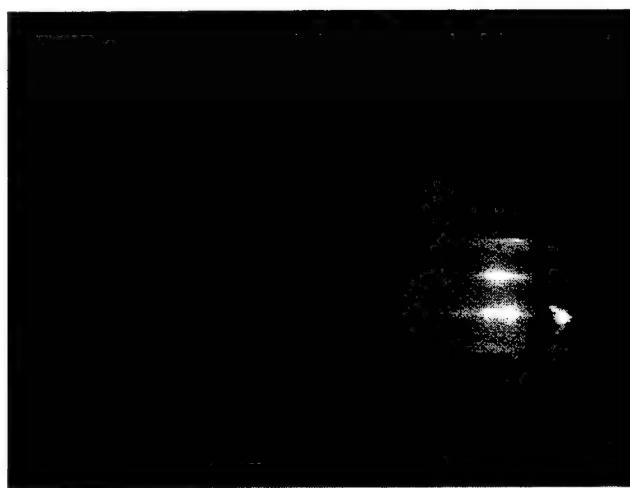

Figure 6: RHEED reconstruction for a sapphire substrate prior to growth of GaN.

to spots. A spotty RHEED pattern indicates that there is surface roughness on more than an atomic scale. A crystal that grows under this condition for extended thickness will likely exhibit defects in crystalline perfection which will be observed with X-Ray diffraction, or electrical and optical properties.

Roughened surfaces with increased layer thickness are often seen for lattice mismatched growth. Rough surfaces have been seen in most GaN growth performed under this effort. Typical RHEED reconstruction at different points in the growth of GaN is seen in Figure 7. Growth initially remains flat as a thin buffer is grown at low temperatures. The low temperature layer is necessary to initiate nucleation. If higher thermocouple temperatures, such as 800°C are used to grow on the bare substrate, no growth will take place, even after several hours of exposure to Ga and atomic nitrogen. Not shown is the RHEED pattern during this initial 700°C growth. It would show that the surface appears to be amorphous after approximately 5-10 monolayers (ML)s. When the growth is interrupted for 2 minutes, the pattern anneals to the form seen in Figure 7. With this very thin layer of growth, the surface seems to be planar and regular. It becomes
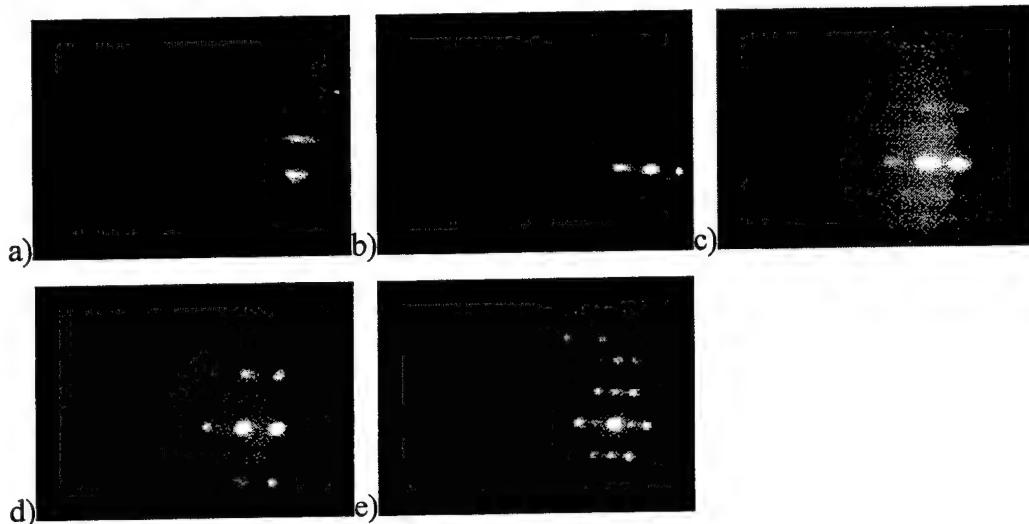
Figure 7: Changes in RHEED pattern during growth of GaN on sapphire using 600W RF power and 1.1×10^{-5} T chamber pressure (wafer GS0091). a) After two monolayers (ML) of growth b) after 2 minutes or 12 MLs of growth with 1 minute interruption c) after an additional 5 minutes of growth prior to anneal d) 240 MLs of growth with temperature raised to 840□C and e) after 0.1 ∓m of GaN growth.

apparent with further growth that the surface becomes rough and somewhat irregular. After just a limited amount of additional growth, the RHEED pattern becomes spotty and remains this way

for any thickness which follows. The spotty growth is presumed to result from rough surfaces caused by the lattice mismatched growth.

This rough surface growth is almost always seen. The exception is when growth conditions are selected which provide insufficient nitrogen overpressure for stoichiometric growth. When the Ga flux is raised to too high of a growth rate, excellent RHEED patterns are seen. The RHEED is streaky and bright which would seem to indicate very good crystal quality. The films, however show large densities of Ga droplets all over the surface. It is not hard to understand how insufficient nitrogen would lead to Ga droplets - excess Ga atoms that migrate on the growing surface would migrate into balls which would continue to grow. It is difficult to understand why the RHEED pattern would look so good. Presumably it indicates that the small GaN islands between the Ga droplets might be of very good quality. There may be some 3D growth taking place free of lattice mismatch dislocations. If so, some form of control of this condition might lead to a better quality crystal. GaN grown with insufficient nitrogen also usually has much stronger photoluminescence quality than films grown without Ga droplets. This characteristic would be desirable for laser application. The density of the droplets, however, is much too high to permit laser device fabrication.

Later in the study it was found the optimum condition for growth was with a V/III ratio nearly equal to unity. The V/III ratio references the number of atomic nitrogen atoms to the number of gallium atoms at the growth surface. This is a difficult parameter to set since it is dependent on several variables including the following: Ga cell temperature, RF plasma power, Nitrogen gas flow rate, and substrate temperature. In addition, a dependence on the thickness of the nucleation layer was seen. This becomes quite complex and repeatability was a problem throughout the study.

GaN Growth Sequence

Due to the severe lattice mismatch of GaN to sapphire, it is impossible to grow a high quality epilayer on sapphire without some method of relieving the strain inherent to mismatched systems. This is accomplished through the use of a low temperature nucleation layer grown between 500-550 degrees Celsius. This layer must be proceeded by a 1-2 minute nitridization step. Nitridization is the exposure of the sapphire surface to the RF nitrogen plasma at a high temperature. The maximum temperature achieved by the system at Cornell was 940 degrees

Celsius. The nitridization is believed to form a thin 10-30 Angstrom layer of AlN on the sapphire which further helps to relieve strain build-up at the epilayer interface.

It was found the optimal thickness of the nucleation layer was between 200-300 Angstroms. Furthermore, a much slower growth rate is necessary at this step to obtain a high quality GaN layer. Growth rates between 0.05-0.10 μm/hr were utilized at this step to provide the best results. Following the nucleation layer, the temperature of the substrate is raised to the mail layer growth temperature between 600-700 degrees Celsius. At this point the V/III ratio must be near unity to obtain high quality films. Typical films grown were between 1-2 microns thick at growth rates from 0.10-0.70 μm/hr. Following this layer all sources were shuttered and the substrate temperature was ramped down to room temperature.

CHARACTERIZATION OF GaN

Atomic Force Microscopy Observations

Early efforts to establish suitable growth conditions for GaN made extensive use of atomic force microscopy (AFM). This technique helped identify useful initial substrate nitriding conditions and buffer growth conditions. It was found through AFM observations that an optimum substrate nitriding condition prior to growth was 3 minutes exposure to atomic nitrogen at 1050°C. Following this step, optimum buffers were established using AFM. Substrate thermocouple temperatures of 700°C permitted nucleation of GaN, while higher temperatures did not. Some AFM images from early growths are seen in Figure 8. In the left image, the surface is a collection of small islands that nucleate together to form GaN. This condition is responsible for the spotty RHEED images seen earlier in this report. In some areas the boundaries of the islands can be seen. These boundaries that appear are the interface defects which exist between the early GaN island nucleation and continue to exist throughout the vertical layer growth of an observed thickness. The electrical and optical properties of these defects are discussed later in this report. The image at right in Figure 8 is somewhat smoother and demonstrates the efforts to improve the quality of material grown. Not shown here is the image of flat films which are grown but show no detail for the purposes of this report. This technique indicated the optimum nucleation temperature was 500 °C.
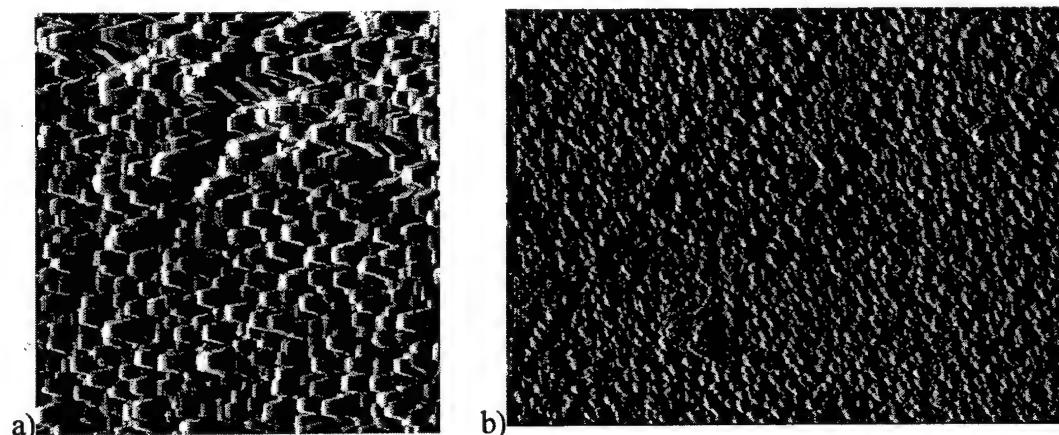

Figure 8: AFM images of GaN grown at Cornell. Image a) represents early growths and attempts to optimize the nucleation layer. Image b) demonstrates improvement in surface quality in follow-on growths.

X-Ray diffraction measurements

X-ray diffraction of GaN is employed to determine the effect of growth conditions on the crystallinity of the grown film. A composite of typical x-ray diffraction patterns is seen in Figure 9. The full width half maximum for GaN far exceeds the sapphire substrate. Even though the x-ray indicates that the GaN is essentially a single crystal, the large diffraction width shows that the crystal is rich in defects resulting from the lattice mismatch with the sapphire substrate. While x-ray widths from some growths are better than that shown here, none are comparable to lattice matched epitaxy to good quality substrates in other materials systems. 24 arcmin was a typical result for most GaN films grown at Cornell. High quality films grown in MOCVD reactors have line widths on the order of 1-2 arcmin. Most MBE grown material is between 10-20 armin.
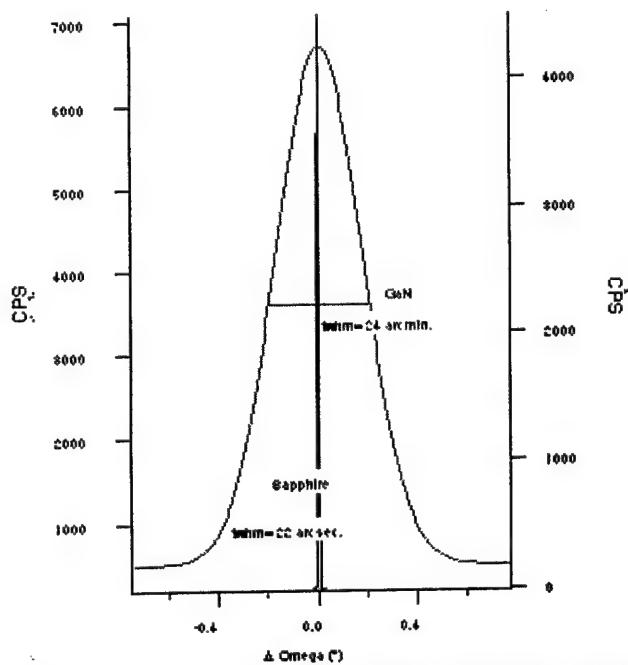
Figure 9: X-ray diffraction patterns comparing a sapphire substrate and GaN grown on top. The center locations have been adjusted for overlap.

Hall Effect Measurements

The electrical properties of GaN need to be optimized for application to devices. High conductivity is desired for low parasitic resistance. Conductivity is proportional to the product of Hall mobility and carrier concentration. Therefore, one goal for GaN used in device applications is to obtain the highest possible doping concentrations at the highest Hall mobility possible. The majority of GaN wafer growths made for this effort were designed to study the effect of growth

conditions on carrier mobility. Some early mobility's for n-type GaN obtained at Cornell and results from elsewhere are seen in Figure 10.

The mobility's follow an inverse square root relationship with doping (carrier) concentration typical of other semiconductors. Mobility's are very high for the highest doped GaN grown at Cornell. These samples doped beyond 1×10^{20} cm^{-3} have the highest conductivity reported in GaN to date. Although the mobility's are approximately 20-40 times lower than those for highly doped GaAs, the doping concentrations are significantly higher than those that can be obtained in GaAs. The product of doping and mobility is therefore slightly higher for GaN than for GaAs. This material should produce very low parasitic resistance in device applications.
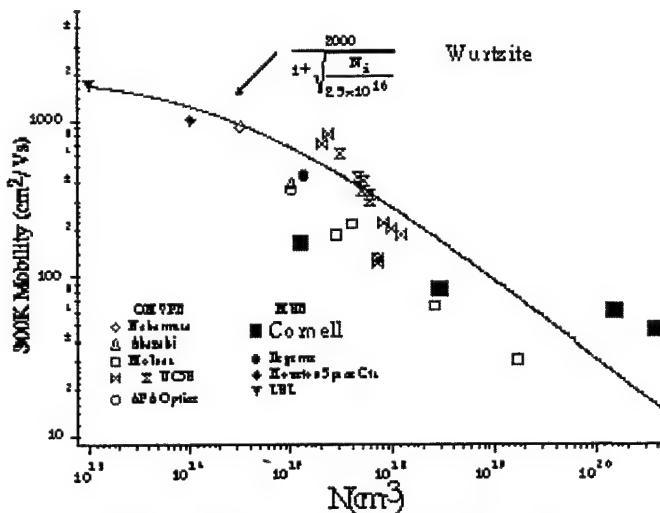
Figure 10: Room temperature Hall mobility as a function of carrier concentration for n-type Wurtzite GaN grown in different laboratories.

The mobility obtained at Cornell at lower doping concentrations are lower than reported in other labs and are a matter of concern. The low mobility's are thought to result from our choice of relatively thin structures for evaluation of doping and mobility studies. The data from this effort shown above are from layers that are 1 micron thick. It is known that mobility in GaN gets higher as thicker layers are grown. Presumably this is the result of defects associated with lattice mismatched growth which are greatest in density near the substrate. A single attempt to grow a thicker layer of 3 microns did not have significantly higher mobility than the 1 micron thick reference. It is not known whether this result is a single anomaly, or is representative of all thicker layers. It is the only thick wafer growth attempted to date.

Another possible explanation for unexpectedly low mobility is scattering from impurities or defects. It is unlikely that ionized impurities exist in significant concentration for these wafers. Shown in Figure 11 is the Si doping calibration data for GaN obtained for 600W plasma power and 0.1 μm/hour growth rate. The curve contains two interesting features. First the curve is linear over a wide range, including at lower doping concentrations. This would not be the case if there were a significant concentration of undoped impurities. In addition, undoped material has higher resistivity and does not exhibit significant concentrations of ionized impurities. Thus, large compensation densities as a cause of low mobility is unlikely. Second the very high doping concentrations that are shown are surprising in this wide bandgap semiconductor. These levels are usually only seen in small bandgap semiconductors, and not even materials such as GaAs exhibit such good doping behavior.
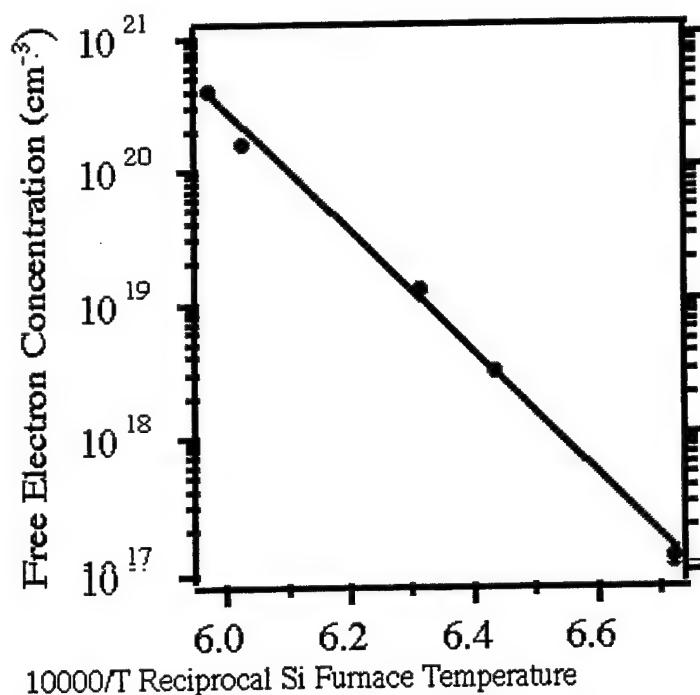

Figure 11: Carrier concentration in n-type GaN as a function of reciprocal temperature of the Si doping furnace.

In contrast to the n-type doping, p doping has proved to be more troublesome. Although a p-type doping curve for Mg in GaAs has been established during this study, it cannot be sure that the few p-type data points for GaN are unambiguous. P-doping of GaN remains a difficult

problem which must be solved for fabrication of lasers and HBTs. Present lateral GaN lasers suffer significant IR drops due to poor p-type GaN doping concentrations.

Films that are grown with a V/III ratio near unity have demonstrated the best electrical characteristics of all other films grown to date. A mobility of 300 cm^2/Vsec at $n=1E10^{17}$ cm^{-3} was achieved with this condition. This proved to be a significant improvement since the highest mobility seen before were at carrier concentrations of $n=1E10^{18}$ cm^{-3}. This improvement was caused due to the reduction in nitrogen vacancies in the epilayer and the improvement in the stoichiometry. The n-type background density is still too high to make low resistance p-type GaN since more than $1E10^{20}$ cm^{-3} concentration of Mg is needed to get $1E10^{18}$ cm^{-3} activated acceptors in the crystal. The reason for less than 1% activation of acceptors is due to the high activation energy of about 250 meV of the Mg acceptor. At room temperature, only 1% of the Mg placed in the crystal is activated as holes.

Photoluminescence Results

Photoluminescence (PL) is an important technique for evaluation of the radiative recombination efficiency of GaN. It has also been used in this study to formulate a model to explain the role of defects arising from lattice mismatched growth. PL from GaN grown at 600W RF plasma power, $2x10^{-5}$ T chamber nitrogen pressure, 840°C substrate temperature (using indium bonded samples) and Si doped to the levels indicated, is shown in Figure 12. The incident laser intensity is very low compared to PL commonly performed on semiconductors. The 20mW laser power is spread over a beam width of approximately 5mm diameter at the surface of the sample. This corresponds to a power density of approximately .01W/cm^2. The low incident power density provides an opportunity to closely examine PL from deep centers within GaN. Since these centers would be expected to saturate and leave only observation of the bound exciton at the band edge at high power densities, low excitation power density permits easy observation of the relationship between deep level filling and band edge luminescence.
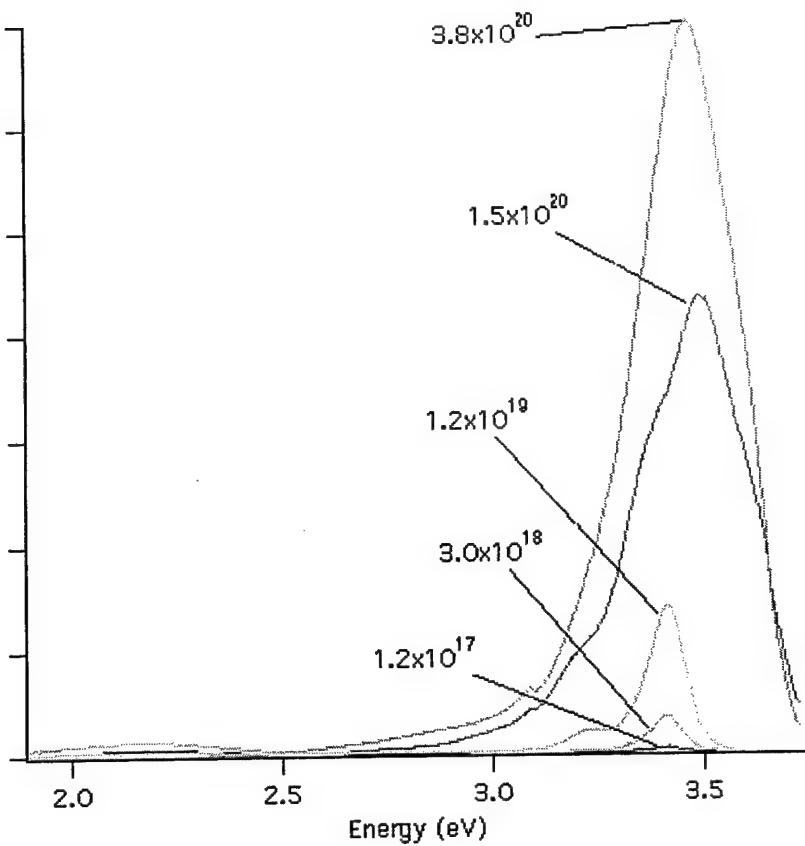
Figure 12: Photoluminescence as a function of n-type carrier concentration. The scale of this plot is linear.

It can be seen that at low doping concentrations, luminescence at yellow wavelengths dominates the PL spectra. Not shown is undoped GaN which has only yellow luminescence and no band edge features at 3.4 eV. As doping concentration is raised, the yellow luminescence falls and band edge luminescence rises. Increased band edge PL with increased doping is not unexpected as the electrons provided by the donors increase the probability of recombination with free holes generated by the incident photons. The decrease in deep level luminescence is not expected for increased doping.

Decreased recombination from the deep level at increased doping concentration can be explained by a model proposed at Cornell. The deep level is modeled to be 2.2eV above the valence band of GaN. The deep level luminescence is from the transition from the deep level to the valence band. The physical origin of the deep level is presumed to be from defects arising from lattice mismatch. These defects are often seen to rise perpendicularly from the substrate

20

interface to the surface. A cross section might appear as simple vertical lines. A schematic showing the band diagram as a function of position and doping levels is seen in Figure 13.
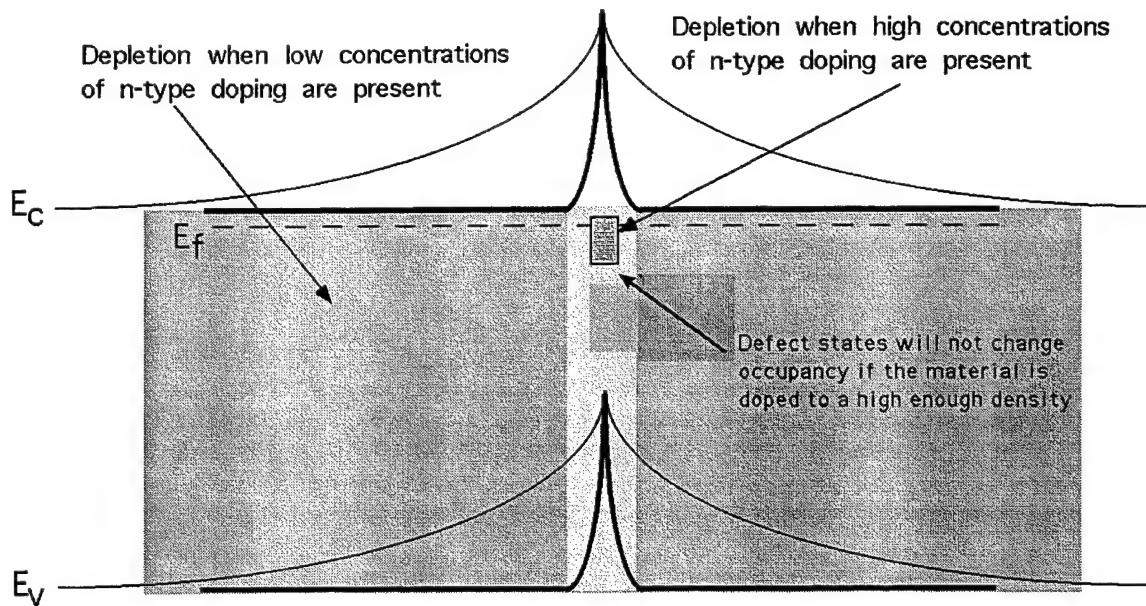

Figure 13: Model of Fermi level pinning by cluster boundary defects in GaN with the effects of doping on the band bending and depletion.

The defect level pins the Fermi-level near mid-gap. The area surrounding the defect is depleted of carriers. If the combination of low doping density and high defect density exists, the material will exhibit very high resistivity. The undoped samples that we have grown at 600W do exhibit high resistivity. Figure 13 also shows the effect of doping on the depletion regions surrounding the defect. Higher doping will result in a much greater fraction of material which is flat-banded and much less material will be depleted surrounding the defect. The probability of band edge luminescence will be highest for the highest doped material, and the probability of luminescence from the defect will be lowest. In addition, the highest doped material will move the Fermi-level above the defect level where it will be completely occupied.

P-type GaN has been grown utilizing magnesium as the dopant. However, only in one case has the mobility of the material been measured by Hall effect. A mobility of 12 cm^2/Vs was measured for the p-type wafer. The difficulty in obtaining high quality p-type GaN is believed to be from large background n-type impurities that occur during growth; thus, the films are compensated and rarely enough to be p-type conductive. The optical properties of as grown p-type material is very promising. Shown in Figure 14 is the room temperature photoluminescence

from a Mg-doped GaN film. The second peak at 386 nm is due to a shallow donor-Mg-acceptor recombination. This spectrum was obtained from a sample that was grown with Mg/Al mixture as the p-type dopant. At the operating temperature for doping of T_{Mg}=350-400 °C the Al is not melted and thus no Al enters the growing crystal. This source was tried because it was thought the Al would act as a filter to getter any Oxygen impurities in the dopant. No proof of this was obtained and when the dopant was switched to pure Mg (4 parts per billion) the quality of the p-type crystal improved.
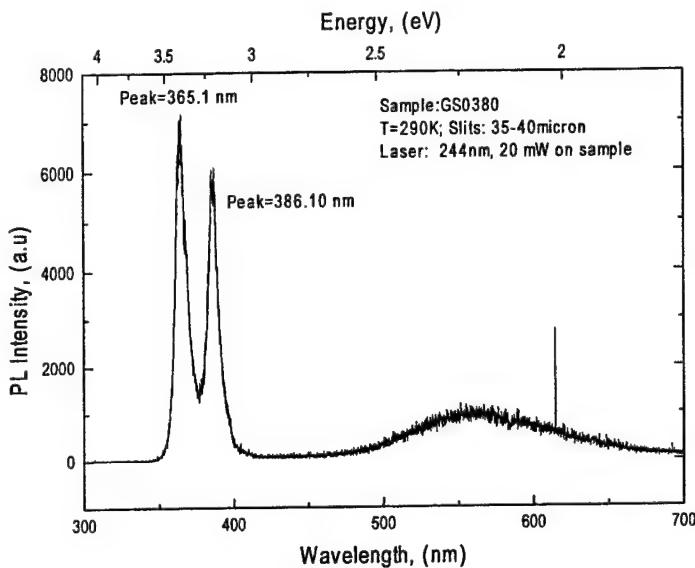
Figure 14: Room temperature PL of Mg-doped GaN. Note weak deep level emissions at 560 nm.

Growth of cubic-GaN

Some effort was directed towards the growth of cubic GaN on cubic SiC. Since cubic GaN is a closer lattice match to cubic SiC, lower defect densities might be expected from growth on this substrate. There would be possible advantages for laser applications using the cubic forms of GaN and AlGaN. The cubic GaN would have cleavage plains closely aligned with the cleavage plains of the substrate. This alignment would allow cleaved facets for high reflectivity mirrors which is vital to laser design. The wavelength ranges available for this material system shown in Figure 1 provide a slightly different band of emission possibilities. There is also some indication that electron mobility might be higher in cubic GaN, due to higher symmetry of the crystal, which would lead to even lower parasitic resistance.

X-ray diffraction of cubic GaN grown on SiC is seen in Figure 15. The cubic peaks for cubic (002) and (004) GaN are clearly visible near the cubic SiC peaks. This result is very encouraging as it shows GaN full width half-maximum values similar to those of the SiC substrate (which is itself grown on Si). Only about 5 growths have been attempted to date on cubic SiC; however, a large supply of substrate has been obtained and many more growths are planned based on the previous growths.
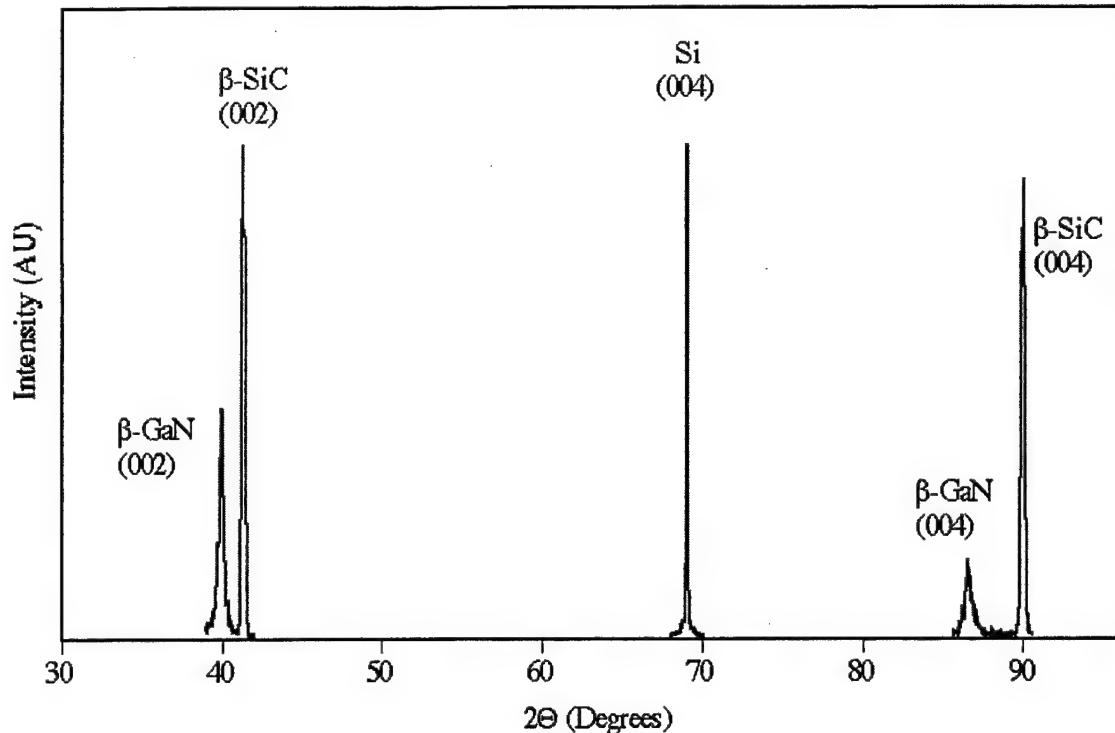
Figure 15: X-ray diffraction of 0.2μm thick cubic GaN grown on SiC at Cornell at 600W RF power.

MATERIAL PROCESSING of GaN

Dry Etching of GaN

The dry etching of III-Nitrides has been reported in various journals. At Cornell, an ECR (Electron Cyclotron Resonance) etcher has primarily been used in GaN etches. An ECR etch was preferred to RIE (Reactive Ion Etch) or Ar Ion Mill, because the etched surfaces using ECR were clean and a clear boundary could be observed between etched and non-etched regions. The possibility of achieving comparable results using RIE or an Ar Ion Mill with process optimization cannot be excluded, though. The additional advantage of ECR is the low damage on

23

Table 1. GaN and Resist Etch rates with Plasma Quest ECR etcher[9]

(RF power: 200 W; Upper Magnet: 16 A; Bottom Magnet: 60A; Resist: SAL 601)

Ar (sccm)	Cl_2 (sccm)	BCl_3 (sccm)	H_2 (sccm)	CH_4 (sccm)	Pressure (mT)	GaN Etch Rate (Å/min)	Resist Etch Rate (Å/min)
10	20	40	10	0	5	1490	1370
10	20	40	10	0	10	1970	2400
10	20	40	10	0	20	960	1680
10	20	40	0	0	10	1200	3500
5	10	20	0	0	5	1155	1330
5	10	0	0	3	5	1820	800

the surface of samples, as ion beams are incident at an angle rather than at a normal direction (90°) to the surface. The side wall shape was not easy to observe among the attempts made as the etch depths were not deep enough. However, as demonstrated by other groups, the vertical side wall can be achieved using ECR. The etch mask was normally SAL 601 -- an electron beam resist. The selectivity of the etch between SAL 601 and the GaN crystal varies according to etch conditions. A problem of using resists as an etch mask is that the resist etch rate is generally much higher than GaN etch rate. SAL 601 demonstrated an advantage on this aspect. The selectivity of up to 1:2 (GaN etches faster) was achieved. Some of the recipes tried and their etch rates are described in Table 1.

Ohmic Contacts on GaN

The performance of GaN devices has been often limited by high contact resistance[10]. Early attempts for better Ohmic contacts include those of Foresi et al.[11] and Lin et al.[12] Foresi et al.[11] employed Al and Au, and achieved about 10^{-3} Ohm-cm^2 after a 575°C anneal for 10 min. Lin et al.[12] adopted a 30 sec 900°C anneal of Ti/Al to achieve a specific contact resistance of $8E10^{-6}$ Ohm-cm^2. Recently Fan et al.[8] realized a very low specific contact resistance of $8.9E10^{-8}$ Ohm-cm^2 utilizing Reactive Ion Etching (RIE) treatment and multi-metal-layers (Ti/Al/Ni/Au).

At Cornell, various types of materials have been tried to obtain good n-type Ohmic contacts. The Ohmic contacts were made in TLM (Transmission Line Model) Patterns on a GaN wafer to determine specific contact resistance. TLM patterns had a set of 7 or 8 metal pads arranged such

24

that the separation between the two adjacent metal pads varied in a regular step size. The separations increased from 5 μm to 35 μm with a step of 5 μm. The TLM patterns are fabricated through etch isolations using the ECR etching and a metal liftoff process. Four point probe method was used to measure the specific contact resistance. Among Ohmic contacts tried, Ti/Al, Ti, AuSi alloy, Ti/Au, and Si implanted contacts yielded reasonable results.

Ti/Au contacts

Though not refractory, Ti/Au contacts, typically 1000 Å Ti and 2000 Å Au, have been a popular choice for many groups. Ti/Au contacts followed by 30 s 750-800°C anneal under N_2 atmosphere yielded about 10^{-3}-10^{-4} Ohm-cm^2.

Ti contacts[13]

A 200 Å Ti layer was employed for Ohmic contacts. The contacts required an annealing to yield smaller contact resistance. The annealing temperature was between 750°C and 850°C for 30 sec. After the annealing more metals were evaporated on the top to facilitate probing. The thickness of 200 Å was a good choice. A 3500 Å Ti contact processed in identical way other than the Ti thickness showed poor results, suggesting the Ti contact may have been obtained through a chemical process. The specific contact resistance of 10^{-3}-10^{-4} Ohm-cm^2 had been achieved.

AuSi alloy contacts

Ni/AuSi/Ag/Au alloy ohmic contact was devised from that of GaAs (Ni/AuGe/Ag/Au). Ni/AuSi/Ag/Au (100 Å/1000 Å/1000 Å/2000 Å) was sequentially evaporated using an electron-beam evaporator. AuSi was a eutectic alloy. Au and Si was evaporated at the same time with dual electron-beams. An annealing time of 30 sec at 750°C gave reasonable contact resistance. The contact resistance was higher than 10^{-3} Ohm-cm^{-2}.

Ti/Au contacts

A Ti adhesion layer of 30 Å followed by Au of 3000 Å for easy probing and low electrical resistance yielded a little high, but comparable contact resistance. No annealing should be followed for this contact, as the annealing degrade the contact resistance. The thickness of Ti was critical. With a thick (300 Å) Ti layer, the contact transformed into a Schottky contact.

Table 2.　　　Si-implantation schedule and simulated projection range calculated by TRIM.[16]

Energy (keV)	Dose (cm^{-2})	Simulated Projection Range (Å)	Simulated Longitudinal Straggling (Å)
30	1E10^{15}	228	128
20	1E10^{15}	143	93
15	1E10^{15}	122	74
10	1E10^{15}	86	55
5	1E10^{15}	50	34

Si implanted contacts

The use of implanted layers has been practiced for GaAs and InP and has also been demonstrated on GaN.[14,15] Growth of the GaN layer was performed in a Varian Gas Source Modular Gen. II MBE (Molecular Beam Epitaxy) system. An Oxford Research RF nitrogen plasma source operating at 600 W was used. Growth occurred on a 1 inch sapphire substrate. An initial GaN buffer layer (~ 250 Å) was grown followed by approximately 1 µm of Si doped GaN. The growth rate was nominally 0.1 µm/hr. The carrier concentration of as-grown wafer was measured by the Hall effect to be $2.2\text{E}10^{16}$ cm^{-3}.

On the grown material mesa isolation was achieved with ECR (Electron Cyclotron Resonance) etching. A mixture of $CH_4/BCl_3/Cl_2/Ar$ was used for the etch. The etch depth was about 1 µm. Si was implanted on portions of the wafer to obtain Ohmic contacts for linear transmission line model (TLM) patterns. The implanted Si was distributed near the surface. The energy, dose, and simulated projection range of the implanted Si are summarized in Table 2.[16]

After the implantation, the sample was annealed in a Rapid Thermal Annealler (RTA) at 1150°C under N_2 atmosphere for 30 sec for the activation of the implanted Si. During the annealing, a GaN wafer was utilized as a cover to prevent possible desorption of the materials. From the simulated results [16], the doping density corresponded to about $2\text{E}10^{21}$ cm^{-3} ($5\text{E}10^{15}$ cm^{-2} doping over ~ 250 Å), assuming 100 % activation of the implanted Si. The surface of the sample was doped higher, as low energy ions spread less (Table 2). From the measured Hall data

of the implanted region after the activation anneal, the doping sheet density was $1.2E10^{15}$ cm^{-2}, indicating an activation efficiency of about 20 %, which roughly corresponded to a bulk density of $4E10^{20}$ cm^{-3}. The charge density of the unimplanted region increased from $2.2E10^{16}$ cm^{-3} to $4E10^{18}$ cm^{-3} after the annealing. This two order of magnitude change in the sheet charge density before and after the 1150°C anneal was attributed to annealing induced defects as pointed out by Chan et al.[15] After the annealing a Ti/Au (30 Å/3000 Å) layer was used as overlay metals across the mesas on top of the Si-implanted regions as well as the unimplanted regions. Ti serves as an adhesion layer. Au provides the electrical contact. No additional annealing was performed after the metals were evaporated. For the contacts on top of the Si-implanted regions, the metals were designed to be set back 1 μm from the boundary of the implanted regions. After the evaporation of the metals, even with an alignment error of about 0.8 μm, the metal contacts were contained on the implanted regions. On the fabricated TLM patterns, resistance was measured using the 4-point probe method with measuring currents between -5 mA and 5 mA. Resistance measured at 5 mA were within 2 % of those measured at zero current. A scanning electron microscope (SEM) was used to measure the distance between individual TLM contacts. An accurate measurement of distances between metal pads is important in determining small specific contact resistance, as the transfer length is significantly small. The measured resistance was plotted as a function of the distance between pads Figure 16. Contact resistance was determined from the intercepts of least square linear fit lines in the resistance-distance plot. The slope for Ti/Au contacts on the unimplanted region was 14 % higher than that on Si-implanted regions. The difference in the slopes was reasonable as the highly conducting Si-implanted regions were extended outside of the metal contact areas. Due to the extremely small contact resistance, some of the contact resistance appeared to be less than zero from experimental errors in determining the intercepts. An average of contact resistance for each measuring current (101 points between -5 mA to 5 mA) was estimated to be -0.0099 Ohm-mm with a standard deviation of 0.097 Ohm-mm. For transfer lengths determined from the ratio of the intercept to the slope of lines in the resistance-distance plot, an average of -0.0043 μm and a standard deviation of 0.046 μm was determined. Both the contact resistance and the transfer length should be positive, but negative numbers with large standard deviations were obtained from the measurements. Using the standard deviations as errors, the maximum specific contact resistance was $3.6E10^{-8}$ Ohm-cm^2. For the unimplanted

27
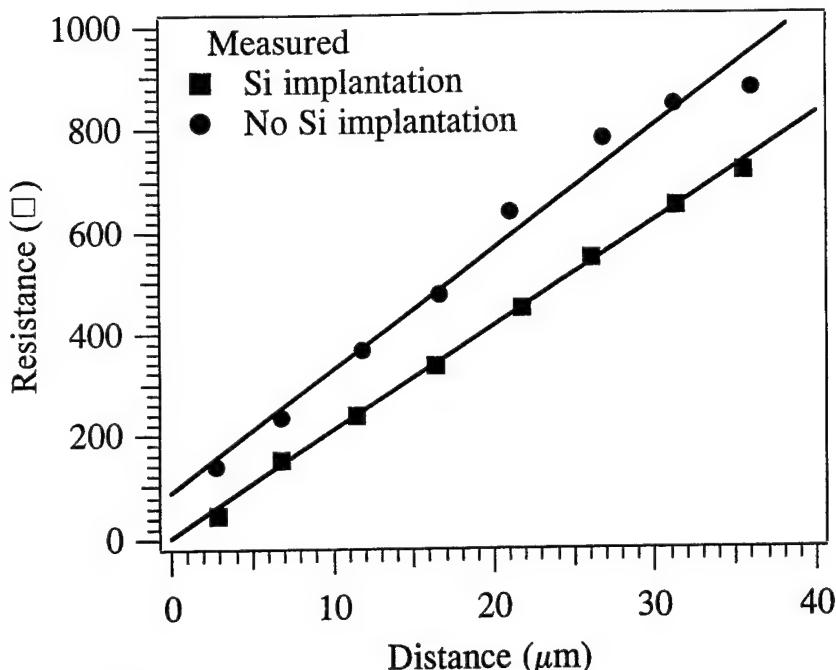
Figure 16: Measured resistance as a function of distance between the metal pads for Si-implanted and unimplanted contacts. Both contacts were made after the annealing of the sample.

contacts on the annealed substrate, the contact resistance was 4.6 Ohm-mm and the transfer length was 2.0 µm, yielding a specific contact resistance of $9.2E10^{-5}$ Ohm-cm^2.

Due to the lack of the material, no quantitative comparison was performed between contacts placed on as-grown GaN and those placed on high temperature annealed GaN. However, a measurement on another wafer showed about a two order of magnitude decrease in the specific contact resistance for the contacts placed on an 1150°C annealed wafer even without Si implantation. This was attributed to an increased carrier density through the annealing process.[15] Besides the Si-implantation, Si diffusion was also attempted. Si films were evaporated on top of GaN films using an electron beam evaporator. The GaN wafer with Si film on was annealed at 1150°C for 30 sec. After the annealing the excess Si was etched from the surface with HF solution. Irregular patterns remained after removing the Si film. The measured sheet charge density was 2.15×10^{13} cm^{-2} for a sample annealed at 1150°C for 1 minute. For a sample annealed at 1050°C for 2 minutes showed 1.17×10^{12} cm^{-2}. The bulk density was not calculated as the Si

28

diffusion depth was not known, but, compared with Si-implanted samples, the sheet charge density was two order of magnitude less, indicating poor Si diffusion and activation.

CONCLUSIONS

An LED structure has not been fabricated in this program. The short term goal of this project was to grow and fabricate blue emitting LEDs based on the current growth techniques developed to date at Cornell. The material quality of the n-type and p-type material is good enough for the growth of an LED. All the pieces have been accomplished; n-and p-type doping, $Al_xGa_{(1-x)}N$ growth, Ohmic contact formation, and dry etching techniques. Unfortunately, the equipment had to be taken off line but good results are expected shortly after restart due two months after this publication.

In addition, the growth of InGaN will be attempted to further increase our capabilities to program the emission wavelength of GaN optical devices. The growth of InN is much more difficult due the differences in growth temperature with GaN. InN prefers lower substrate temperatures compared to GaN. With InGaN/GaN quantum wells, the emission wavelength of an LED structure can be made between 370-400 nm and possibly further. However, the effects of lattice mismatch and temperature effects must be overcome to reach beyond 400 nm without the use of n-and p-type dopants in the active region.

For the realization of III-nitride based light generating devices, processing techniques have been experimented. The etching of the III-V nitride have been performed mainly with dry etch using ECR etcher. Various etch rates were achieved with different etching conditions. The developed etching has been utilized in device isolations. The various n-type ohmic contact was studied. The contact resistance varied depending on the states of the wafers, such as doping density and quality of crystals. Among the contacts experimented Ti/Al, Ti, Ti/Au, AuSi alloy contact, and Si-implanted contact yielded reasonable results.

For the realization of high performance light generating devices, p-type contact should be investigated. Due to the relatively high acceptor energy levels in III-V nitride, the activation efficiency of accepts is low to begin with. The reported p-type contacts includes Au[17], Ni/Au[1], and Au/Mg[18]. For the realization of smooth side walls, dry etching technique needs to be investigated further. The quality of dry etched side walls depends not only on etch conditions,

29

such as types of gas used, pressure, and RF power, but etch mask qualities, as edge patterns of masks will be transferred into side wall profile. Ideal etch masks should process high etch selectivity between III-V nitrides and the etch masks and should be removed easily once etching has been done.

MBE is still a viable method to grow GaN, but progress has been much slower than that seen in Metal-Organic or Vapor Phase techniques. To date, all blue LD's that have been made have been grown by vapor phase techniques. The growth of GaN by the vapor transport techniques has been ongoing for over 20 years now, which places MBE at a disadvantage. Many more lessons must be learned in order to overcome the problems associated with MBE. Sufficient atomic nitrogen incident on the growing wafer leads the list of problems to overcome.

REFERENCES

[1] S. Nakamura, M. Senoh, S-i Nagahama, N. Iwasa, T. Yamada, T. Matsushita, H. Kiyoku and Y. Sugimoto, "InGaN-Based Multi-Quantum-Well-Structure Laser Diodes," Jpn. J. Appl. Phys., vol. 35, pp. L74-L76, 1996.

[2] I. Akasaki, S. Sota, H. Sakai, T. Tanaka, M. Koike and H. Amano, "Shortest wavelength semiconductor laser diode", Electron. Lett., vol. 32, pp. 1105-1106, 1996.

[3] S. Nakamura, M. Senoh, N. Iwasa, and S.-i. Nagahama, "High-power InGaN single-quantum-well-structure blue and violet light-emitting diodes," Appl. Phys. Lett., vol. 67, pp. 1868-1870, 1995.

[4] M. A. Khan, Q. Chen, M. S. Shur, B. T. Dermott, J. A. Higgins, J. Burm, W. Schaff, and L. F. Eastman, "Short-channel GaN/AlGaN doped channel heterostructure field effect transistors with 36.1 cutoff frequency," Electron. Lett., vol. 32, pp. 357-358, 1996.

[5] J. Burm, W. J. Schaff, and L. F. Eastman, H. Amano, and I. Akasaki, "75 Å GaN channel Modulation Doped Field Effect Transistors," Appl. Phys. Lett., vol. 68, pp. 2849-2851 (1996).

[6] J. R. Mileham, S. J. Pearton, C. R. Abernathy, J. D. MacKenzie, R. J. Shul, and S. P. Kilcoyne, "Wet chemical etching of AlN," Appl. Phys. Lett., vol. 67, pp.1119-1121, 1995.

[7] S. M. Sze, Physics of Semiconductor Devices, 2nd Ed., 304, John Wiley & Sons (1981).

[8] Z. Fan, S. N. Mohammad, W. Kim, Ö. Aktas, A. E. Botchkarev, and H. Morkoç, Appl. Phys. Lett. **68** 1672 (1996).

[9] R. Michalak, Private Communication

[10] M. A. Khan, J. N. Kuznia, D. T. Olson, W. J. Schaff, J. Burm, and M. S. Shur Appl. Phys. Lett. 65 1121 (1994).

[11] J. S. Foresi and T. D. Moustakas, Appl. Phys. Lett. 62 2859, (1993).

[12] M. E. Lin, Z. Ma, F. Y. Huang, Z. F. Fan, L. H. Allen, and H. Morkoç, *Appl. Phys. Lett.* **64**, 1003 (1994).

[13] M. Umesh, Private Communication

[14] J. C. Zolper, R. J. Shul, A. G. Baca, R. G. Wilson, S. J. Pearton, R. A. Stall, *Appl. Phys. Lett.* **68** 2273 (1996).

[15] J. S. Chan, N. W. Cheung, L. Schloss, E. Jones, W. S. Wong, N. Newman, X. Liu, E. R. Weber, A. Grossman, and M. D. Rubin, *Appl. Phys. Lett.* **68** 2702 (1996).

[16] J. F. Ziegler, TRansport of Ions in Matter (TRIM), ver. 92.12, IBM-Research, Yorktown, NY (1992).

[17] S. Nakamura, M. Senoh, and T. Mukai, Jpn. J. Appl. Phys. Pt. 2 **32** L8 (1993).

[18] L.L. Smith, M.D. Bremser, E.P. Carlson, T.W. Weeks, Jr, Y. Huang, M.J. Kim, R.W. Carpenter, R.F. Davis,Gallium Nitride and Related Materials. First International Symposium, p. 861-6 (1996).A problem to overcome in achieving high performance GaN-based devices is the realization of good reliable metal contacts.